

β -D-GALACTOPYRANOSIDE *SECO*-PHYTOPORPHYRIN FROM *ATROPA BELLADONNA* AND *SOLANUM TUBEROSUM* YELLOW LEAVES DETERMINED BY NUCLEAR MAGNETIC RESONANCE

Nina Djapic

Technical Faculty "Mihajlo Pupin", University of Novi Sad, Djure Djakovica bb, Zrenjanin 23000, Serbia
e-mail: nidjapic@gmail.com

Abstract: The screening for the presence of a chlorophyll catabolite in two Solanaceae plant species yellow leaves was positive, revealing the possibility for its isolation. The purification of the methanol extract from the yellow leaves of *Atropa belladonna* and *Solanum tuberosum* using column chromatography revealed the presence of chlorophyll catabolite glycoside. The chlorophyll catabolite structure was determined through 1D and 2D NMR spectral data analysis, showing that both Solanaceae plant species yellow leaves contain the β -D-galactopyranoside *seco*-phytoporphyrin.

Keywords: chlorophyll catabolite, structure, nuclear magnetic resonance, *Atropa belladonna*, *Solanum tuberosum*.

Received: 26 July 2021/ Revised final: 26 November 2021/ Accepted: 27 November 2021

Introduction

The nuances from green to yellow colours in leaves are mostly due to the structure, stereochemistry and equilibrium forms of the chlorophylls. Considerable investigations have been done to determine the chemical composition of the Solanaceae plant leaves. Limited information is available regarding the chlorophyll catabolite content in Solanaceae leaves, most investigations concern the alkaloid content. All *Atropa belladonna* plant parts, including leaves, contain alkaloids atropine, hyoscyne and scopolamine making them poisonous [1]. *Solanum tuberosum* is an important crop producing tubers in high yields, used in nutrition. The starch in *S. tuberosum* leaves was previously investigated, and it was found that its content depends on the photoperiod treatment [2-4]. The method for identification of organic acids present in *S. tuberosum* leaves has been developed opening the possibility to study their profile during the vegetative period [5,6]. The nitrogen containing compounds found in *S. tuberosum* leaves are glycoalkaloids: α -solanine and α -chaconine [7,8]. Amino acids and amides content in *S. tuberosum* leaves decrease with senescence while the calcium, magnesium and manganese concentrations increase with senescence [9,10]. The decline in photosynthetic rate is associated with leaf aging and the chlorophyll content [11]. The photosynthesis rate in *S. tuberosum* leaves

was measured and it depends on the photoperiod and environmental conditions [12,13]. The investigations on the industrial crop *Nicotiana tabacum*, yellow leaves are more numerous than on the yellow leaves of *A. belladonna* and *S. tuberosum*. In the neutral aroma constituents of Burley tobacco two pyrroles were identified, the indole and *N*-methyl-maleimide, and one imide, methylethyl-maleimide [14]. Two pyrroles were constituents of volatile flavour compounds from tobacco leaf: 2-formylpyrrole and 2-formyl-5-methylpyrrole [15]. The origin of pyrroles and imide could be attributed to pyrolysis or a biochemical process [15].

The scope of this paper was to investigate the structure of naturally occurring chlorophyll catabolites in yellow leaves of *A. belladonna* and *S. tuberosum* var. cultivar Rudolph, Solanaceae. In higher plants, chlorophylls undergo the biodegradation to various *seco*-phytoporphyrins. Further biodegradation compounds of *seco*-phytoporphyrins are unknown, up to now. The investigations aim to resolve the fate of four nitrogen atoms of the chlorophyll molecule. Nitrogen is a growth-limiting element in plants and the storage form of four nitrogen atoms from chlorophylls in the hibernating parts of the plant is still unknown. An approach to resolve only the *seco*-phytoporphyrin present in two Solanaceae species yellow leaves is described in this study.

Experimental

Materials

Methanol (CH₃OH) and dichloromethane (CH₂Cl₂) of p.a. grade, and silica gel 60 were obtained from Centrohem, Stara Pazova, Serbia. The 99.8% deuterated methanol (CD₃OD) was obtained from Carl Roth GmbH&Co KG, Karlsruhe, Germany.

Atropa belladonna yellow leaves were collected from the local greenwood nursery in August 2019. The *Solanum tuberosum* var. cultivar Rudolph yellow leaves were collected at the end of August 2019 in the fields by the river Tisa, Banat side, Serbia.

Methods

Chlorophyll catabolite extraction procedure

The leaves were grinded in a rotating blade grinder Bosch MKM 6003 (Stuttgart, Germany). The chlorophyll catabolite, for every plant species separately, was extracted from 250 g (fresh weight) grinded plant material with 500 mL of CH₃OH in a beaker followed by the sample suspension filtration and concentration in a rotary evaporator (Rotavapor[®] R-300, Buchi, Flawil, Switzerland) to 1 mL volume of the resulting sample (t < 40°C). The chlorophyll catabolite isolation was done by the preparatory open column chromatography. Separation was carried out on a 50x500 mm glass column packed with silica gel. Afterwards, the CH₂Cl₂ was used as the eluent. The study showed that 250 mL of CH₂Cl₂ were not sufficient to complete the separation of a slightly polar fractions and the elution continued with 250 mL CH₂Cl₂:CH₃OH (1:2 v/v). The 50 mL collected fractions were concentrated in a rotary evaporator (t < 40°C). A quantity of 2.12 mg of the pure *A. belladonna* chlorophyll catabolite and 1.73 mg of the pure *S. tuberosum* chlorophyll catabolite was obtained. The samples were dried under vacuum and used for recording nuclear magnetic resonance (NMR) spectra.

The dry weights were determined by placing 1 g of grinded leaves in 10 cm³ pre-weighed clean and dry beakers. The samples were then dried in an oven (Sutjeska, Serbia) at 105°C for 24 hours, followed by cooling in a desiccator for 60 minutes prior to the weight determination. The weight was determined on the analytical balance (Mettler Toledo, XS105 DualRange, Greifensee, Switzerland). The water content 12.35±0.12% and 11.97±0.09% in samples from *A. belladonna* and *S. tuberosum*, respectively.

Spectroscopic measurements

UV-Vis spectra were recorded on a Hach DR6000TM UV-Vis spectrophotometer (Loveland, Colorado, USA).

The mass spectra were recorded on a Bruker Daltonics apex IV FTMS (Bremen, Germany). Samples were analysed by electrospray ionization mass spectrometry (ESI-MS). Samples were dissolved in CH₃OH and directly infused in the ESI source from a syringe pump. The capillary voltage was 4500 V. Mass spectrometer was operating in a positive mode.

NMR spectra were recorded at 500.13 MHz for ¹H and 1D NOE (Nuclear Overhauser Effect) difference experiments and 125.75 MHz for ¹³C on a Bruker Avance DRX 500 NMR (Bremen, Germany) using standard Bruker pulse sequence [16]. The COSY (COrrrelation SpectroscopY) experiment provided the means of identifying mutually coupled protons; the spectrum was acquired with a relaxation delay $d_1 = 2$ s; 2048 data points for f_2 , 16 transients and 512 increments, linear prediction to 2048 points for f_1 . The HSQC (Heteronuclear Single Quantum Coherence) experiment was used to determine proton carbon single bond correlations, where the protons laid along the f_2 (X) axis and the carbons along the f_1 (Y) axis. The HSQC spectrum was acquired with the relaxation delay $d_1 = 2$ s; 2048 data points for f_2 , 16 transients and 512 increments, linear prediction to 2048 points for f_1 . The HMBC (Heteronuclear Multiple Bond Correlation) experiment gave correlations between carbons and proton that are separated by two and three bonds. The HMBC spectrum was obtained under the same acquisition as the HSQC; 1024 data points for f_2 , linear prediction to 1024 points for f_1 [17,18]. The pure compounds were dissolved in CD₃OD prior to NMR measurements. The measurements were done at 25.0±0.5°C. The temperature was controlled by Bruker B-VT 1000 temperature control device. The spectra were recorded in a 5.0 mm inverse detection microprobe head (see Supplementary Material). Chemical shifts are presented relatively to tetramethylsilane (TMS) at δ 0.00. The ACD Labs software was used for the NMR data analysis.

Seco-phytoporphyrin from *A. belladonna*. Amorphous solid. UV-Vis (C = 1·10⁻⁸ mol/L in CH₃OH): λ_{\max} [nm] (log ϵ) to be 244 (7.23) and 312 (7.01). HRESIMS m/z 807.3451 for C₄₁H₅₀N₄O₁₃ [M+H]⁺. ¹H NMR [ppm] δ 4.01 (1H, dd, $J = 4.6, 8.4$ Hz, H-1), 1.97 (3H, s, CH₃-2¹), 6.44 (1H, dd, $J = 11.7, 17.7$ Hz, H_X-3¹), 5.35 (1H, dd, $J = 2.4, 11.7$ Hz, H_A-3²), 6.09 (1H, dd, $J = 2.4, 17.7$ Hz, H_M-3²), 9.30 (1H, s, H-5), 2.23 (3H, s, CH₃-7¹), 2.67 (1H, ddd, $J = 1.8, 7.2, 12.9$ Hz, H_A-8¹), 3.45 (1H, ddd, $J = 2.2, 7.0, 12.9$ Hz, H_B-8¹), 2.70 (1H, ddd, $J = 2.2, 7.1, 11.5$ Hz, H_A-8²), 3.62 (1H, ddd, $J = 1.9, 6.8, 11.9$ Hz,

H_B-8²), 3.97 (2H, d, *J* = 2.6 Hz, H-10), 2.12 (3H, s, CH₃-12¹), 3.78 (1H, t, *J* = 2.3, H-13²), 3.76 (3H, s, CH₃-13⁴), 4.91 (1H, d, *J* = 2.4, H-15), 2.36 (1H, dd, *J* = 6.5, 14.4 Hz, H_A-17¹), 2.64 (1H, dd, *J* = 6.6, 14.5 Hz, H_B-17¹), 2.26 (1H, dd, *J* = 6.8, 13.3 Hz, H_A-17²), 2.29 (1H, dd, *J* = 6.6, 13.0 Hz, H_B-17²), 1.91 (3H, s, CH₃-18¹), 2.87 (1H, dd, *J* = 5.0, 14.7 Hz, H_A-20), 2.47 (1H, dd, *J* = 9.0, 14.5 Hz, H_B-20), 4.19 (1H, d, *J* = 7.8 Hz, H-1'), 3.16 (1H, dd, *J* = 7.8, 9.2 Hz, H-2'), 3.33 (1H, dt, *J* = 9.5, 4.1 Hz, H-3'), 3.24 (1H, dd, *J* = 4.0, 4.5 Hz, H-4'), 3.85 (1H, ddd, *J* = 4.4, 2.4, 6.6 Hz, H-5'), 3.64 (1H, dd, *J* = 2.6, 11.9 Hz, H_A-6'), 3.80 (1H, dd, *J* = 6.8, 11.9 Hz, H_B-6'). ¹³C NMR [ppm] δ_C 61.5 (C-1), 156.0 (C-2), 12.5 (C-2¹), 128.7 (C-3), 127.1 (C-3¹), 119.0 (C-3²), 174.5 (C-4), 178.0 (C-5), 129.1 (C-6), 135.2 (C-7), 8.7 (C-7¹), 121.1 (C-8), 24.9 (C-8¹), 70.3 (C-8²), 139.2 (C-9), 23.7 (C-10), 133.8 (C-11), 112.9 (C-12), 9.2 (C-12¹), 125.7 (C-13), 194.8 (C-13¹), 67.7 (C-13²), 171.5 (C-13³), 52.6 (C-13⁴), 161.0 (C-14), 37.2 (C-15), 125.1 (C-16), 120.2 (C-17), 20.8 (C-17¹), 37.2 (C-17²), 177.9 (C-17³), 114.7 (C-18), 9.0 (C-18¹), 124.7 (C-19), 29.7 (C-20), 103.6 (C-1'), 72.0 (C-2'), 75.0 (C-3'), 70.2 (C-4'), 78.0 (C-5'), 62.5 (C-6').

Seco-phytoporphyrin from *S. tuberosum*. Amorphous solid. UV-Vis (C = 1·10⁻⁸ mol/L in CH₃OH): λ_{max} [nm] (log ε) to be 244 (7.23) and 312 (7.01). HRESIMS *m/z* 807.3451 for C₄₁H₅₀N₄O₁₃ [M+H]⁺. ¹H NMR [ppm] δ 4.01 (1H, dd, *J* = 4.6, 8.4 Hz, H-1), 1.97 (3H, s, CH₃-2¹), 6.44 (1H, dd, *J* = 11.7, 17.7 Hz, H_X-3¹), 5.35 (1H, dd, *J* = 2.4, 11.7 Hz, H_A-3²), 6.09 (1H, dd, *J* = 2.4, 17.7 Hz, H_M-3²), 9.30 (1H, s, H-5), 2.23 (3H, s, CH₃-7¹), 2.67 (1H, ddd, *J* = 1.8, 7.2, 12.8 Hz, H_A-8¹), 3.45 (1H, ddd, *J* = 2.2, 7.1, 12.9 Hz, H_B-8¹), 2.70 (1H, ddd, *J* = 2.2, 7.1, 11.5 Hz, H_A-8²), 3.62 (1H, ddd, *J* = 1.9, 6.8, 11.9 Hz, H_B-8²), 3.97 (2H, d, *J* = 2.6 Hz, H-10), 2.12 (3H, s, CH₃-12¹), 3.78 (1H, t, *J* = 2.3, H-13²), 3.76 (3H, s, CH₃-13⁴), 4.91 (1H, d, *J* = 2.4, H-15), 2.36 (1H, dd, *J* = 6.5, 14.4 Hz, H_A-17¹), 2.64 (1H, dd, *J* = 6.6, 14.5 Hz, H_B-17¹), 2.26 (1H, dd, *J* = 6.8, 13.3 Hz, H_A-17²), 2.29 (1H, dd, *J* = 6.6, 13.0 Hz, H_B-17²), 1.91 (3H, s, CH₃-18¹), 2.87 (1H, dd, *J* = 5.0, 14.7 Hz, H_A-20), 2.47 (1H, dd, *J* = 9.0, 14.5 Hz, H_B-20), 4.19 (1H, d, *J* = 7.8 Hz, H-1'), 3.16 (1H, dd, *J* = 7.8, 9.2 Hz, H-2'), 3.33 (1H, dt, *J* = 9.3, 4.0 Hz, H-3'), 3.24 (1H, dd, *J* = 4.2, 4.6 Hz, H-4'), 3.85 (1H, ddd, *J* = 4.6, 2.6, 6.7 Hz, H-5'), 3.64 (1H, dd, *J* = 2.7, 11.9 Hz, H_A-6'), 3.80 (1H, dd, *J* = 6.8, 11.9 Hz, H_B-6'). ¹³C NMR [ppm] δ_C 61.5 (C-1), 156.0 (C-2), 12.5 (C-2¹), 128.7 (C-3), 127.1 (C-3¹), 119.0 (C-3²), 174.5 (C-4), 178.0 (C-5), 129.1 (C-6), 135.2 (C-7), 8.7 (C-7¹), 121.1 (C-8), 24.9

(C-8¹), 70.3 (C-8²), 139.2 (C-9), 23.7 (C-10), 133.8 (C-11), 112.9 (C-12), 9.2 (C-12¹), 125.7 (C-13), 194.8 (C-13¹), 67.7 (C-13²), 171.5 (C-13³), 52.6 (C-13⁴), 161.0 (C-14), 37.2 (C-15), 125.1 (C-16), 120.2 (C-17), 20.8 (C-17¹), 37.2 (C-17²), 177.9 (C-17³), 114.7 (C-18), 9.0 (C-18¹), 124.7 (C-19), 29.7 (C-20), 103.6 (C-1'), 72.0 (C-2'), 75.0 (C-3'), 70.2 (C-4'), 78.0 (C-5'), 62.5 (C-6').

Results and discussion

Yellow leaves of *A. belladonna* and *S. tuberosum* were used for the extraction of *seco*-phytoporphyrins in order to find their bioavailability and determine their structure. The recorded UV-Vis spectra presented two distinctive bands of absorption, at 244 nm and 312 nm (Figure S9). The absorption peak at 312 nm belongs to the pyrrole ring bearing the β-D-galactopyranoside unit. The absorption band at 244 nm can belong to 4-methyl-3-vinyl-1H-pyrrol-2-one attached to a methylene bridge that links the consecutive pyrrole ring in the molecule or to the 3-methyl-1H-pyrrole fused to the ring that bears methyl-acetate and oxo group. The band at 205 nm from the UV-Vis spectrum is attributed to CH₃OH, which was used as solvent. The ESI-MS spectrum revealed the ion peak at *m/z* 807.3451 corresponding to the molecular formula C₄₁H₅₀N₄O₁₃ for the [M+H]⁺ ion, this was supported by the NMR spectra recorded.

Isolated samples were dissolved in CD₃OD and NMR spectra were recorded. The isolated tetrapyrrole can be named according to the rules of organic chemistry nomenclature [19]. The name is extremely long and for the time being, the chlorophyll catabolite will be named β-D-galactopyranoside *seco*-phytoporphyrin. The integration of signals in the ¹H NMR spectrum revealed the presence of 32 protons (Figure S1). The -OH and -NH protons exchanged with deuterium in deuterated CD₃OD solvent and were not present in the ¹H spectrum. The low-field singlet at 9.30 ppm was assigned to H-5 aldehyde proton. The three low field *doublet of doublets* signals indicated the presence of one AMX spin-splitting pattern. The 17.9 Hz coupling constant indicated *trans*-coplanar arrangement for H_M and H_X protons. Protons H_A and H_X had a coupling constant of 11.7 Hz. The 2.4 Hz coupling constant suggested geminal positions of H_A and H_M protons. The NOE experiment revealed the methyl group in the vicinity (Figure S7). Then, the -CH₃-2¹ signal at 1.97 ppm had the enhancement after the irradiation of the H_X-3¹ proton. The H-1 proton constituted a spin system

identified with the *doublet of doublets* ($J= 4.6$ and 8.4 Hz) at 4.01 ppm. When the *doublet of doublets* at 4.01 ppm was selectively irradiated the pair of *doublet of doublets* at 2.87 ppm and 2.47 ppm were enhanced indicating the H_{A-20} and H_{B-20} methylene bridge protons. The integration of the *doublet* at 3.97 ppm indicated the presence of two protons. After their selective irradiation, the methylene bridge protons at the position 10 were revealed. The irradiation of the signal at 3.78 ppm enhanced the signals at 3.76 ppm and 4.91 ppm permitting the attribution of $H-13^2$ to the chemical shift of 3.78 ppm, the methoxycarbonyl group CO_2Me-13^4 with the *singlet* at 3.76 ppm and further the 4.91 ppm to $H-15$, respectively. The H_A-17^1 , H_B-17^1 and H_A-17^2 , H_B-17^2 protons of the propionyl side chain constituted a four-spin system which was identified in a form of *doublet of doublets* at 2.36 , 2.64 , 2.26 and 2.29 ppm, respectively [20]. The selective irradiation of the signal at 2.64 ppm resolved the neighbouring methyl group at 1.91 ppm to be CH_3-18^1 (Figure S8). The H_A-8^1 , H_B-8^1 and H_A-8^2 , H_B-8^2 protons constituted a four-spin *doublet of doublets of doublets* system with chemical shifts at 2.67 , 3.45 , 2.70 and 3.62 ppm, respectively. The selective irradiation of the signal at 3.45 ppm enhanced the signal at 2.23 ppm indicating the methyl group CH_3-7^1 . The anomeric sugar proton in chlorophyll catabolite *O*-glycoside was at 4.19 ppm. Other sugar ring protons were positioned in the narrow spectral region from 3.16 to 3.84 ppm. The anomeric proton signal appeared at 4.19 ppm *doublet* ($H-1'$, $J= 7.8$ Hz). In pyranose form, the $^3J_{(HH)}$ between the ring protons reflect the angle between the investigated protons. The $^3J_{(HH)}$ coupling constants can be used in the identification of glycoside unit, the anomeric configuration and conformational analysis of the sugar ring. The coupling constant of 7.8 Hz between the anomeric proton and the $H-2'$ proton of the galactose unit showed the β -configuration at the anomeric center corresponding to β -D-galactopyranose. The signal at 3.16 ppm had a coupling constant of $J= 7.8$ and 9.2 Hz indicating the $H-2'$ position. The $H-3'$ proton had a coupling constant of $J= 9.5$ and 4.1 Hz revealing its position at 3.33 ppm. The equatorial proton $H-4'$ ($J= 4.0$ Hz) had the coupling with the axial $H-3'$ and with the axial $H-5'$ the coupling was $J= 4.5$ Hz. The $H-5'$ had scalar coupling with $H-4'$, H_A-6' and H_B-6' . The H_A-6' and H_B-6' had a coupling constant of 11.9 Hz. The H_A-6' was coupled with $H-5'$ with the $J= 2.6$ Hz indicating the geminal position of H_A-6' and $H-5'$ protons. By the selective

decoupling of $H-1'$ at 4.19 ppm the enhanced was one *doublet of triplets* at 3.33 ppm, the *doublet of doublets of doublets* at 3.85 ppm, the *doublet of doublets of doublets* at 2.70 ppm and the *doublet of doublets of doublets* at 3.62 ppm indicating the 4C_1 conformation. The H_A-6' and H_B-6' signals were found at 3.64 ppm and 3.80 ppm, respectively, due to their connection to the same carbon after observation of a $H_A-6'/C-6'$ and $H_B-6'/C-6'$ correlation in the HSQC experiment (Figure S5).

The COSY spectrum revealed the arrangement of proton-proton connectivities (Figure S3). The downfield H_B-3^2 vinyl proton was assigned to geminal H_A-3^2 tracing further to vicinal $H-3^1$ proton. The next connectivity network started from the further downfield aliphatic proton $H-1$ resonating at 4.01 ppm and it had strong off-diagonal correlating signals with H_A-20 and H_B-20 spin system. Then, the next analysed strongly coupled spin system was propionyl side chain with geminal coupling constants of 14.5 Hz and aliphatic vicinal couplings of 7.5 Hz. The $H-17^2$ protons had off-diagonal response to their neighbouring H_A-17^1 and H_B-17^1 protons. The ethylene group protons H_A-8^2 and H_B-8^2 had off-diagonal signals with neighbouring H_A-8^1 and H_B-8^1 protons. In the sugar unit, it was possible to follow the sequential 'walk' starting from the anomeric proton $H-1'$ signal through the entire sugar unit (Figure S4). The 2D COSY spectrum, magnified in the region of sugar protons, gave the insight to scalarly coupled protons. In the COSY spectrum there was a strong correlation signal between $H-1'$ and $H-2'$; $H-3'$ and $H-4'$; $H-4'$ and $H-5'$; $H-5'$ and H_A-6' ; H_A-6' and H_B-6' indicating a significant scalar coupling between these protons. The starting point for the assignment was a *doublet* at 4.19 ppm corresponding to the $H-1'$ proton. In the 2D COSY correlation map, the H,H spin coupling was observed with a signal at 3.16 ppm belonging to the $H-2'$ proton. The $H-2'$ proton then had an off-diagonal response with a signal at 3.33 ppm permitting the assignment of that signal to the $H-3'$ proton. Continuing further in the contour map, the $H-3'$ proton had an off-diagonal response with a signal at 3.24 ppm indicating the $H-4'$. In the contour map, the signal at 3.85 ppm had an off-diagonal response with $H-4'$, thus indicating to the $H-5'$ proton. The $H-5'$ proton had an off-diagonal response with the proton resonating at 3.64 ppm that was assigned to H_A-6' . The H_A-6' had an off-diagonal response with the signal at 3.80 ppm revealing the H_B-6' .

After the assignment of all chlorophyll catabolite proton signals, the carbon signals were designated from heteronuclear single quantum correlation (HSQC) two-dimensional spectrum revealing the directly connected proton-carbon pairs (Figure S5). The nonequivalent geminal methylene protons in the propionyl and ethylene side chain were easily observed. Methylene bridge carbons had the difference in chemical shifts of 6 ppm and were nonequivalent. In the vinyl region the C-3² had a cross peak with H_A-3² and H_M-3² protons. The long range HMBC correlation map established the connectivities in the tetrapyrrole ring system (Figure S6). The most upfield methyl group resonating at 1.91 ppm had connectivities to three carbons resonating at 120.2, 114.7 and 124.7 ppm identifying three quaternary carbons C-17, C-18 and C-19, respectively. The H-3¹ had connectivities with C-2, C-3 and C-3². The connectivities of the C-7¹ methyl group provided the information about the positions of C-8 and C-8¹. Further in the clockwise direction, H-10 protons revealed the connectivity with four quaternary carbons C-8, C-9, C-11 and C-12. The proton H_A-17¹ resonating at 2.36 ppm established the key connectivity. The proton was related to C-16, C-17, C-18, C-17² and C-17³ linking the pieces of the propionyl side chain together. The anomeric proton H-1' had a connectivity with C-8², C-2' and C-3'. The H_A-6' had a connectivity with C-5' and C-4'. The pyranose form was determined from the ¹³C-shift values. In furanoses, the carbon-shifts of the ring carbons are shifted considerably downfield [21]. Spectral data provided the means to assemble the complete structure of **1** (Figure 1).

The structure of chlorophyll catabolite isolated from *S. tuberosum* yellow leaves, analysed by ¹H NMR (Figure S2) had the same signal pattern in the spectrum as that met in the ¹H NMR spectrum of *A. belladonna* chlorophyll catabolite. The ¹H NMR spectrum signals of chlorophyll catabolite isolated from *S. tuberosum* var. Rudolph yellow leaves can be subdivided into well-separated regions. Starting from the low field the protons on heteroatoms and aldehyde proton are positioned. The protons on heteroatoms exchanged with deuterium leaving in the low field region only the aldehyde proton at 9.30 ppm. The vinyl side chain protons were in the chemical shifts region 5.35 ppm to 6.44 ppm with the characteristic coupling patterns revealing the AMX spin splitting system. The tetrapyrrole ring bears three protons resonating at 3.78 ppm, 4.01 ppm and 4.91 ppm. The proton resonating at 3.78 ppm slowly exchanged; this can be attributed to the keto-enol tautomerization and deuterio exchange. The anomeric sugar protons came in the spectral region from 4.19 ppm, for the anomeric proton H-1' to 3.16 ppm for H-2'. The number of signals in this region indicated one sugar unit. From the obtained NMR spectra, it was concluded that the chlorophyll catabolite has a sugar unit in a form of β-D-galactopyranoside. The NOE spectra recorded revealed the ⁴C₁ conformation of the sugar unit. The obtained results determined that the sugar structure registered in the analysed sample is the β-D-galactopyranoside. In the low field region were recorded the signals of the side chain groups: propionyl, ethylenyl and methyl. The methylene bridge protons were resonating in the low field region.

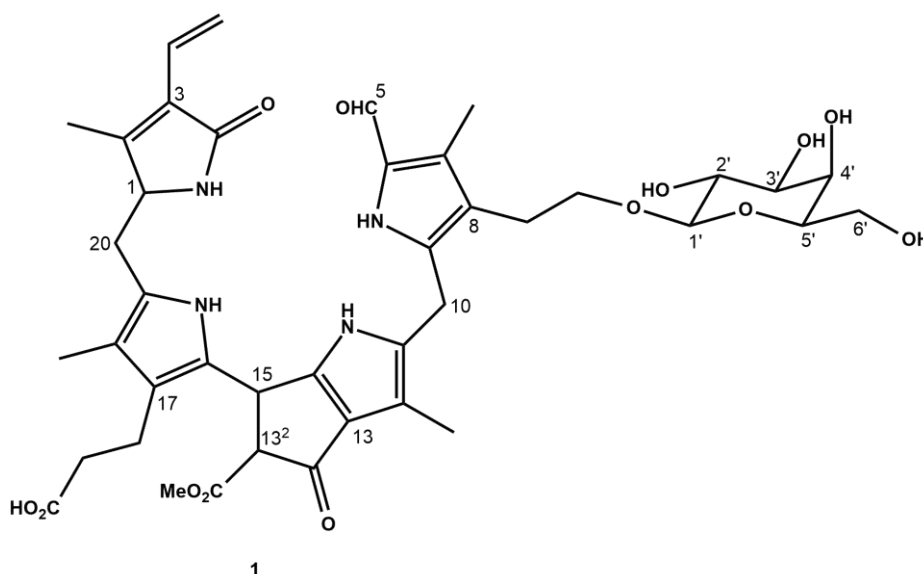


Figure 1. Chlorophyll catabolite structure isolated from *A. belladonna* and *S. tuberosum*.

The only slight differences between the *A. belladonna* and *S. tuberosum* chlorophyll catabolite were the coupling constants values. The obtained spectra for the *S. tuberosum* chlorophyll catabolite were identical to the spectra for the *A. belladonna* chlorophyll catabolite indicating that the same chlorophyll catabolite exists in both plant species yellow leaves.

Further investigations of the Solanaceae plant species yellow leaves can reveal whether the whole plant family has the same chlorophyll catabolite.

Conclusions

The study described the isolation of β -D-galactopyranoside *seco*-phytyporphyrin from *A. belladonna* and *S. tuberosum* yellow leaves. Column chromatography was applied for its isolation. The UV-Vis, mass spectrometry and NMR spectroscopy were used for the structure confirmation.

The obtained results by means of nuclear magnetic resonance have shown that the two plant species from Solanaceae plant family contain the same chlorophyll catabolite in yellow leaves. There are only infinitesimal differences in coupling constants. It was demonstrated that the configuration on chiral carbons is the same indicating that the same enzymes are present in the analysed yellow leaves extracts from both Solanaceae plant species. Thus, that senescent autumnal leaves could be considered as valuable sources for the isolation of *seco*-phytyporphyrins.

Supplementary information

Supplementary data are available free of charge at <http://ejm.asm.md> as PDF file.

References

- Kohnen-Johannsen, K.L.; Kayser, O. Tropane alkaloids: chemistry, pharmacology, biosynthesis and production. *Molecules*, 2019, 24(4), 796, pp. 1-23. DOI: <https://doi.org/10.3390/molecules24040796>
- Lorenzen, J.H.; Ewing, E.E. Starch accumulation in leaves of potato (*Solanum tuberosum* L.) during the first 18 days of photoperiod treatment. *Annals of Botany*, 1992, 69(6), pp. 481-485. DOI: <https://doi.org/10.1093/oxfordjournals.aob.a088375>
- Santacruz, S.; Koch, K.; Andersson, R.; Aman, P. Characterization of potato leaf starch. *Journal of Agricultural and Food Chemistry*, 2004, 52(7), pp. 1985-1989. DOI: <https://doi.org/10.1021/jf030601k>
- Hovenkamp-Hermelink, J.H.M.; De Vries, J.N.; Adamse, P.; Jacobsen, E.; Witholt, B.; Feenstra, W.J. Rapid estimation of the amylose/amylopectin ratio in small amounts of tuber and leaf tissue of the potato. *Potato Research*, 1988, 31, pp. 241-246. DOI: <https://doi.org/10.1007/BF02365532>
- Rodriguez-Perez, C.; Gomez-Caravaca, A.M.; Guerra-Hernandez, E.; Cerretani, L.; Garcia-Villanova, B.; Verardo, V. Comprehensive metabolite profiling of *Solanum tuberosum* L. (potato) leaves by HPLC-ESI-QTOF-MS. *Food Research International*, 2018, 112, pp. 390-399. DOI: <https://doi.org/10.1016/j.foodres.2018.06.060>
- Odgerel, K.; Banfalvi, Z. Metabolite analysis of tubers and leaves of two potato cultivars and their grafts. *PLOS ONE*, 2021, 16(5), e0250858, pp. 1-14. DOI: <https://doi.org/10.1371/journal.pone.0250858>
- Dao, L.; Friedman, M. Comparison of glycoalkaloid content of fresh and freeze-dried potato leaves determined by HPLC and colorimetry. *Journal of Agricultural and Food Chemistry*, 1996, 44(8), pp. 2287-2291. DOI: <https://doi.org/10.1021/jf9502820>
- Brown, M.S.; McDonald, G.M.; Friedman, M. Sampling leaves of young potato (*Solanum tuberosum*) plants for glycoalkaloid analysis. *Journal of Agricultural and Food Chemistry*, 1999, 47(6), pp. 2331-2334. DOI: <https://doi.org/10.1021/jf981124m>
- Millard, P.; Marshall, B. Growth, nitrogen uptake and partitioning within the potato (*Solanum tuberosum* L.) crop, in relation to nitrogen application. *The Journal of Agricultural Sciences, Cambridge Core*, 1986, 107(2), pp. 421-429. DOI: <https://doi.org/10.1017/S0021859600087220>
- Kolbe, H.; Stephan-Beckmann, S. Development, growth and chemical composition of the potato crop (*Solanum tuberosum* L.). II. Tuber and whole plant. *Potato Research* 1997, 40, pp. 135-153. DOI: <https://doi.org/10.1007/BF02358240>
- Olesinski, A.A.; Wolf, S.; Rudich, J.; Marani, A. Effect of leaf age and shading on photosynthesis in potatoes (*Solanum tuberosum*). *Annals of Botany*, 1989, 64(6), pp. 643-650. DOI: <https://doi.org/10.1093/oxfordjournals.aob.a087889>
- Frier, V. The relationship between photosynthesis and tuber growth in *Solanum tuberosum* L. *Journal of Experimental Botany*, 1977, 28(4), pp. 999-1007. DOI: <https://doi.org/10.1093/jxb/28.4.999>
- Vos, J.; Oyarzun, P.J. Photosynthesis and stomatal conductance of potato leaves-effects of leaf age, irradiance, and leaf water potential. *Photosynthesis Research* 1987, 11, pp. 253-264. DOI: <https://doi.org/10.1007/BF00055065>
- Fujimori, T.; Kasuga, R.; Matsushita, H.; Kaneko, H.; Noguchi, M. Neutral aroma constituents in Burley Tobacco. *Agricultural and Biological Chemistry*, 1976, 40(2), pp. 303-315. DOI: <https://doi.org/10.1080/00021369.1976.10862038>
- Yokoi, M.; Shimoda, M. Extraction of volatile flavour compounds from tobacco leaf through a low-density polyethylene membrane. *Journal of Chromatographic Science*, 2017, 55(3), pp. 373-377. DOI: <https://doi.org/10.1093/chromsci/bmw178>

16. Braun, S.; Kalinowski, H.-O.; Berger, S. 150 and more basic NMR experiments: practical course. Wiley: VCH, Weinheim, 1998, 610 p. <https://www.wiley-vch.de/en/>
17. Smith, K.M.; Goff, D.A.; Abraham, R.J. The NMR spectra of porphyrins. 27-proton NMR spectra of chlorophyll-*a* and pheophytin-*a*. Organic Magnetic Resonance, 1984, 22(12), pp. 779-783. DOI: <https://doi.org/10.1002/mrc.1270221210>
18. Andersen, Ø.M.; Fossen, T. Characterization of anthocyanins by NMR. Current protocols in food analytical chemistry, 2003, 9(1), F1.4.1-F1.4.23, pp. 1-23. DOI: <https://doi.org/10.1002/0471142913.faf0104s09>
19. Hellwich, K.-H.; Hartshorn, R.M.; Yerin, A.; Damhus, T; Hutton, A.T. Brief guide to the nomenclature of organic chemistry (IUPAC Technical Report). Pure and Applied Chemistry, 2020, 92(3), pp. 527-539. DOI: <https://doi.org/10.1515/pac-2019-0104>
20. Smith, K.M.; Goff, D.A.; Abraham, R.J. NMR spectra of porphyrins. 29. Conformation of the propionic ester side chain in chlorophyll derivatives. The Journal of Organic Chemistry, 1987, 52(2), pp. 176-180. DOI: <https://doi.org/10.1021/jo00378a003>
21. Beier, R.C.; Mundy, B.P.; Strobel, G.A. Assignment of anomeric configuration and identification of carbohydrate residues by ¹³C NMR. 1. Galacto- and glucopyranosides and furanosides. Canadian Journal of Chemistry, 1980, 58(24), pp. 2800-2804. DOI: <https://doi.org/10.1139/v80-448>